Fischer–Tropsch synthesis: Kinetics and water effect study over 25%Co/Al2O3 catalysts

ARTICLE *in* CATALYSIS TODAY · JUNE 2014

Impact Factor: 3.31 · DOI: 10.1016/j.cattod.2013.10.014

7 AUTHORS, INCLUDING:

Wenping ma
University of Kentucky
75 PUBLICATIONS **448** CITATIONS
SEE PROFILE

Burtron Davis
University of Kentucky
548 PUBLICATIONS **7,889** CITATIONS
SEE PROFILE

Jennifer L.S. Klettlinger
Kennedy Space Center
13 PUBLICATIONS **40** CITATIONS
SEE PROFILE

Catalysis Today 228 (2014) 158–166

Contents lists available at ScienceDirect

Catalysis Today

journal homepage: www.elsevier.com/locate/cattod

Fischer–Tropsch synthesis: Kinetics and water effect study over 25%Co/Al_2O_3 catalysts

Wenping Ma[a], Gary Jacobs[a], Dennis E. Sparks[a], Robert L. Spicer[a], Burtron H. Davis[a,*], Jennifer L.S. Klettlinger[b], Chia H. Yen[b]

[a] Center for Applied Energy Research, University of Kentucky, 2540 Research Park Drive, Lexington, KY 40511, USA
[b] NASA Glenn Research Center, 21000 Brookpark Road, Cleveland, OH 44135, USA

ARTICLE INFO

Article history:
Received 25 June 2013
Received in revised form
30 September 2013
Accepted 4 October 2013
Available online 5 November 2013

Keywords:
Fischer–Tropsch synthesis
Kinetics
Kinetic water effect
Co/Al_2O_3

ABSTRACT

The kinetics of Fischer–Tropsch synthesis (FTS) over a 25%Co/Al_2O_3 catalyst was studied using a 1-L continuously stirred tank reactor (CSTR) under the conditions of 205–230 °C, 1.4–2.5 MPa, H_2/CO = 1.0–2.5 and 3–16 NL/g-cat/h (X_{CO} = 7–54%). Thirty-one sets of kinetic data collected at 220 °C with a low extent of deactivation were used for kinetic parameter regression. The CAER empirical kinetic model ($r_{FT} = kP_{CO}^{a}P_{H_2}^{b}/(1 + mP_{H_2O}/P_{H_2})$) was employed to study the kinetic effect of water. A positive kinetic water effect was first evidenced using the kinetic approach, consistent with the results of the effect of co-fed water on cobalt FTS in this work and the literature (e.g. Loegdberg et al., 2011 [21]) for Co/Al_2O_3 catalysts. The current kinetic results are based on kinetic data taken following an initial catalyst induction period, where the CO conversion had stabilized. These data are different from our earlier investigations where reversible oxidation of small cobalt crystallites and/or catalyst support effects likely impacted the cobalt site densities, resulting in a negative water effect. Thus, in this study, we decoupled the effect of reversible oxidation from the kinetics, so that the effect of water on stable (i.e., presumably larger) metallic cobalt particles could be assessed.

In this study, an additional eleven classical FT kinetic models for Co catalysts were tested using the kinetic data. Five of them were also found to adequately describe the kinetic data, including two mechanistic models developed based on carbide mechanisms. The CAER model containing a water effect term and the mechanistic model of Botes et al. (2009) [31] yielded comparable reaction orders for the partial pressures of H_2 and CO, resulted in a better fit of the kinetic data.

1. Introduction

Supported cobalt catalysts have received renewed attention in converting natural gas or biomass to liquid transportation fuels through the Fischer–Tropsch synthesis (FTS) reaction, due to their high activity and high selectivity toward heavier hydrocarbons [1–4]. The kinetics of FTS on cobalt-based catalysts has also gained renewed focus, and many kinetic studies over cobalt catalysts using either fixed-bed or slurry phase reactors have emerged [5–20]. Despite this, consensus for a particular FTS kinetic model has not been attained. Moreover, issues regarding how water impacts FTS kinetics are still being debated. Several groups have reported that water plays a kinetic role in FTS for both Co and Fe catalysts [1,5,6,19,21,22], while others have reported that the role of water during FTS is negligible [13–18,23]. Additional studies are thus needed to resolve these issues.

To accurately measure the kinetic behavior of a FTS catalyst, it is necessary to obtain kinetic data at steady state conditions with a low degree of catalyst deactivation. One reason is that the nature of the active site may be altered if the catalyst undergoes a high extent of deactivation during the kinetic experiment. For example, catalyst cluster size changes have been reported to affect the activity and selectivity [24–27] and change in catalyst surface energetics can influence adsorption and desorption behavior, especially after the catalyst surface becomes oxidized or covered with carbon [26]. From the standpoint of reactor performance, product compositions usually change during deactivation, and this leads to errors in the calculated kinetic parameter values [13]. While the deactivation of cobalt FTS catalysts is unavoidable, the rate of change of deactivation should be kept to a minimum during kinetic studies. A subtle consequence of this is that stable periods of testing follow an initial rapid decay period; thus, stable periods useful for kinetic evaluation occur on a catalyst that has already experienced significant deactivation. Deactivation is perhaps the main reason why FTS kinetic studies for cobalt catalysts remain so challenging. Achieving a set of kinetic data for a catalytic test during which little additional deactivation (or negligible further deactivation) occurs

* Corresponding author. Tel.: +1 859 257 0251; fax: +1 859 257 0302.
E-mail address: burtron.davis@uky.edu (B.H. Davis).

0920-5861/$ – see front matter © 2013 Elsevier B.V. All rights reserved.
http://dx.doi.org/10.1016/j.cattod.2013.10.014

is highly desired for selecting proper cobalt kinetic models and accurately determining kinetic parameters. So far, among many reported Co FTS kinetic studies, few have addressed the issue of catalyst deactivation experienced during kinetic studies [5,6,13].

In our group, preliminary studies of the kinetics of FTS over a Co/Al_2O_3 catalyst have been conducted under constant partial pressures of CO and H_2 and constant temperature [5,6]. The extent of catalyst deactivation during kinetic experiments was in the range of 50–70%, and the catalyst activity was corrected to that of a fresh catalyst basis for calculating kinetic parameters; this was accomplished by assuming that cobalt site time yield is constant for any surface cobalt site and that losses in catalyst activity were only due to losses in cobalt active sites. The CAER empirical kinetic model that was developed is:

$$r_{FT} = \frac{kP_{CO}^{a}P_{H_2}^{b}}{1 + mP_{H_2O}/P_{H_2}}. \quad (1)$$

This equation was used to obtain the kinetic effect of water. Kinetic results of the studies suggested a negative kinetic water effect on Co/Al_2O_3 catalyst activity and the reaction orders obtained in the two studies were comparable (−0.2 to −0.3 for P_{CO}, and 0.5–0.6 for P_{H_2}) [5,6]. However, in a recent study [21], a positive water effect for a Co/Al_2O_3 catalyst was reported. Thus, it is necessary to conduct additional studies to shed light on the reasons for this difference. In this study, we aim to obtain kinetic data during periods where the rate of change of catalytic activity is low. This occurs following the initial catalyst induction period, and aims to minimize the impact of reversible oxidation due to small crystallites present in the fresh catalyst earlier in the test as well as other induction impacts. Consequently kinetic parameters, such as the kinetic effect of water, can be quantified for the more stable cobalt metal particles (i.e., presumably larger after aging and more resistant to reversible oxidation) and an appropriate kinetic model chosen, preferably one that reflects important aspects of the FTS mechanism occurring on metallic cobalt sites. That is, our aim is to decouple any positive impact of water occurring on stable metallic cobalt particles from the negative reversible effect of water occurring on small unstable cobalt crystallites.

2. Experimental

2.1. Catalyst preparation

A slurry impregnation method was employed to load cobalt onto the alumina support. The support was Catalox SBA 150 γ-Al_2O_3 (150 m^2/g) and cobalt nitrate was used as the precursor. The volume of the impregnated cobalt nitrate solution was controlled by adjusting the ratio of the volume of solution to the weight of alumina to 1:1, such that approximately 2.5 times the pore volume of the solution was used to prepare the catalysts. Due to the solubility limit of cobalt nitrate in water, two slurry impregnations were required. After each impregnation, the catalyst was dried under vacuum in a rotary evaporator at 80–100 °C. Ru promoter, when used, was added by incipient wetness impregnation following cobalt addition and ruthenium nitrosyl nitrate was the precursor salt. The final dried catalyst was calcined in flowing air for 4 h at 350 °C. The surface area of the final calcined 25%Co/Al_2O_3 catalysts, with or without promoters, was about 105 m^2/g. The Co cluster size was determined to be 13.3 nm for the unpromoted 25%Co/Al_2O_3 catalyst and 11.0 nm for the Ru promoted 25%Co/Al_2O_3 catalyst.

2.2. Catalyst pretreatment

The 25%Co/Al_2O_3 catalyst (~10 g) was ground and sieved to 45–90 μm before loading into a fixed-bed reactor for 10 h of ex situ reduction at 350 °C and atmospheric pressure using a gas mixture of H_2/He with a molar ratio of 1:3. The reduced catalyst was then cooled and transferred into a 1-L CSTR under the protection of N_2. The CSTR was previously charged with 315 g of Polywax 3000 and heated until the slurry medium was melt. The CSTR was sealed and purged with N_2 gas (30 NL/h) for 2 h before injecting catalysts. The transferred cobalt catalysts were further reduced in situ at 230 °C at atmospheric pressure using pure hydrogen for another 10 h before starting the FTS reaction.

2.3. Kinetic experiment and kinetic data

The kinetic experiments were carried out over the 25%Co/Al_2O_3 catalyst for a range of conditions in a 1-L CSTR: 205–230 °C, 1.4–2.5 MPa, H_2/CO ratio of 1.0–2.5 and space velocity of 3–16 NL/g-cat/h. Two sets of data with constant partial pressures of CO or H_2 were obtained. Reference conditions (220 °C, 1.8 MPa, H_2/CO ratio of 2.5 and space velocity of 8.8 NL/g-cat/h) were frequently returned to during the experiment in order to assess the extent of catalyst deactivation. In total, 42 experimental conditions yielding CO conversions below 60% at 220 °C were conducted. During kinetic data analysis, only 31 of the 42 sets of conditions were used, since the first five and the last six sets of experimental data had excessive catalyst deactivation. Table 1 summarizes the experimental conditions and FTS rate results. The mass balance period for each set of conditions was between 8 and 25 h. The total and element mass balances for the kinetic data fall in the range of 100 ± 4.0%. In addition, we obtained 2–3 data points at 205, 213 and 230 °C by the end of the run in order to determine activation energy using an Arrhenius plot.

2.4. Water co-feeding experiment

To experimentally determine the kinetic effect of water during FTS, water co-feeding experiments were also performed over a 0.27%Ru–25%Co/Al_2O_3 catalyst using a 1-L CSTR. Since the additional added water may suppress CO conversion (i.e., either temporarily or permanently) through the oxidation of small cobalt crystallites, which could impact the kinetic water effect for the cobalt catalyst [21,23,31], attempts were made to minimize cobalt site suppression by water reoxidation. One approach is to use low to medium water concentrations in the feed and a short water feeding period, so that the aspects of the water effect on kinetics can be measured when reversible and/or irreversible catalyst deactivation during water feeding is negligible. To do this, a high gas flow rate was applied so that a constant value for the FTS vapor products after changing conditions can be reached as quickly as possible. In this study, the addition of 10% water in syngas (v/v) was carried out at a low CO conversion (19%) by using a high inlet syngas flow rate (157 NL/h). Such high flow rates allow the vapor phase in the reactor to attain a steady state within 0.5–0.7 h. The added water was introduced using a high pressure precision syringe pump (ISCO 500 D). The syngas pressure and syngas flow rate were maintained constant during water addition. The constant syngas pressure was maintained by increasing the total pressure by 10% to compensate for the difference that results by feeding 10% water. The addition of water was continued for 2 h and gas sampling was performed about every 20 min. After the termination of water addition, a new steady state was achieved in about 1.0 h, at which point the CO conversion and selectivities to CH_4 and CO_2 essentially returned to the original values before water addition, implying that 2 h of addition of 10% water did not measurably deactivate the cobalt catalyst.

Table 1
Kinetic conditions and experimental and predicted FTS rates over 25% Co/Al_2O_3 (220 °C).

Run number	TOS (h)	P_{CO}, MPa	P_{H_2}, MPa	H_2:CO	SV, NL/g-cat/h	y_i [a]			r_{FT}, mol/g-cat/h	
						H_2	CO	H_2O	Experimental	Calculated
1[b]	365.42	0.511	1.278	2.5	8.8	0.671	0.258	0.059	0.0212	0.0206
2	384.00	0.710	1.420	2.0	16.0	0.646	0.322	0.026	0.0205	0.0202
3	416.67		1.420	2.0	10.0	0.629	0.316	0.047	0.0207	0.0199
4	431.33		1.420	2.0	6.0	0.601	0.304	0.082	0.0204	0.0196
5	440.17		1.420	2.0	3.0	0.514	0.268	0.191	0.0188	0.0186
6[b]	461.08			2.5	8.8	0.674	0.259	0.055	0.0203	0.0207
7	481.25		1.065	1.5	16.0	0.581	0.394	0.021	0.0178	0.0157
8	503.67		1.065	1.5	10.0	0.565	0.394	0.036	0.0151	0.0154
9	513.75		1.065	1.5	3.0	0.471	0.378	0.134	0.0129	0.0138
10	527.17		1.065	1.5	6.0	0.540	0.390	0.061	0.0145	0.0149
11[b]	550.58			2.5	8.8	0.675	0.261	0.053	0.0204	0.0205
12	562.25		0.710	1.0	16.0	0.478	0.504	0.015	0.0100	0.0109
13	575.17		0.710	1.0	10.0	0.466	0.501	0.027	0.0112	0.0107
14	585.67		0.710	1.0	3.0	0.391	0.501	0.097	0.0099	0.0095
15	601.00		0.710	1.0	6.0	0.451	0.499	0.045	0.0111	0.0105
16[b]	625.00			2.5	8.8	0.675	0.262	0.052	0.0207	0.0206
17	647.83	0.487	1.217	2.5	16.0	0.695	0.273	0.027	0.0226	0.0202
18	671.52	0.487		2.5	10.0	0.679	0.265	0.046	0.0206	0.0200
19	681.75	0.487		2.5	3.0	0.557	0.192	0.216	0.0199	0.0198
20	694.92	0.487		2.5	6.0	0.652	0.250	0.083	0.0192	0.0199
21[b]	719.17			2.5	8.8	0.671	0.260	0.058	0.0200	0.0205
22	743.33	0.608		2.0	16.0	0.645	0.325	0.025	0.0175	0.0185
23	773.08	0.608		2.0	10.0	0.630	0.318	0.044	0.0172	0.0184
24	791.17	0.608		2.0	6.0	0.601	0.309	0.077	0.0175	0.0180
25	801.42	0.608		2.0	3.0	0.521	0.272	0.181	0.0182	0.0172
26[b]	818.17			2.5	8.8	0.674	0.263	0.053	0.0196	0.0205
27	839.83	0.811		1.5	16.0	0.579	0.395	0.022	0.0157	0.0168
28	863.50	0.811		1.5	10.0	0.568	0.389	0.037	0.0184	0.0166
29	888.50	0.811		1.5	6.0	0.539	0.388	0.063	0.0148	0.0160
30	901.58	0.811		1.5	3.0	0.471	0.375	0.137	0.0141	0.0148
31[b]	918.75			2.5	8.8	0.675	0.264	0.051	0.0192	0.0205

[a] y_i = moles of ith specie in the vapor in the reactor/total moles of unreacted syngas, organics and water in the vapor in the reactor.
[b] Repeated experiment.

Table 2
Kinetic results of 25%Co/Al_2O_3 at 220 °C for the CAER model.

Model	Parameter values				Statistical values		
	k, mol/g-cat/h/MPa$^{(a+b)}$	a	b	m	F[a]	R^2	RMSE
$(r_{FT}) = kP_{CO}^{a}P_{H_2}^{b}/(1 + mP_{H_2O}/P_{H_2})$	0.0133	−0.31	0.88	−0.24	1.73	0.950	7.60E−04
t-Value[b]	41.6	−8.1	14.9	−2.9			

[a] $F_{26,6} = 3.83$.
[b] $t_{critical(0.95,\,4,\,31)} = 1.70$.

2.5. Parameter estimation and model discrimination

The FTS kinetic models utilized in this study are shown in Table 2. The kinetic parameters at 220 °C for different models were estimated using the nonlinear least squares fitting method (Levenberg–Marquart) by minimizing the objective function defined in Eq. (2):

$$F_{obj} = \sum_{1}^{N_{exp}} [(r_{FT} - \hat{r}_{FT})]^2 \quad (2)$$

where r_{FT} and $\hat{r}_{FT}$ are experimental and calculated FT rates, respectively. Model discrimination was performed on the basis of statistical significance measured by F values, R square values (R^2) and root mean square error (RMSE) and physical meaning of the parameters. These were computed based on the following equations:

$$F = \frac{(SSR - \sigma^2 \times n_i)/(n - p - n_i)}{\sigma^2} \quad (3)$$

$$R^2 = 1 - \left(\frac{SSR}{SST}\right) \quad (4)$$

$$RMSE = \sqrt{\frac{\sum_{1}^{N_{exp}} [(r_{FT} - \hat{r}_{FT})]^2}{n}} \quad (5)$$

where SSR is the sum of squared residuals, SST is the sum of squares about the mean, n is the number of independent rate data points, p is the number of parameters, n_i is the number of degrees associated with replications at each point for the independent variable, and σ^2 is the pure error variance obtained from repeated experimental rates. Models to provide a satisfactory fit of the data are indicated by model F values being less than critical F-values at a certain probability level (for example, 5%) for rejection, a low RMSE and an R^2 approaching unity.

The Arrhenius activation energy for hydrocarbon formation was determined by plotting ln(k) vs. $1/T$ using the data recorded at 220 °C and data collected at 205, 213 and 230 °C.

3. Results and discussion

3.1. Catalyst activity at baseline conditions

Kinetic experiments for an air calcined 25%Co/Al_2O_3 catalyst were performed over a wide range of reaction conditions as

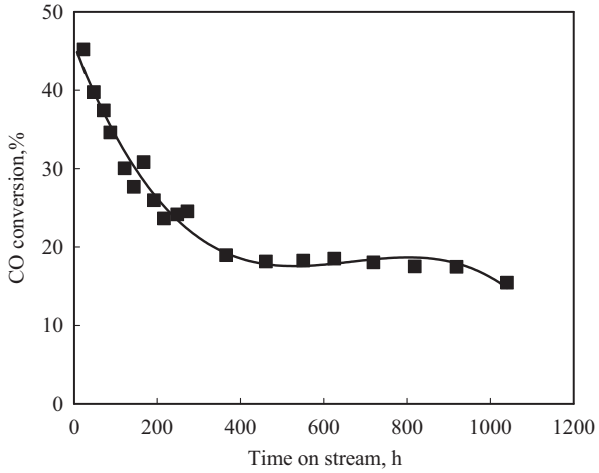

Fig. 1. CO conversion as a function of time over 25%Co/γ-Al_2O_3 (220 °C, 1.84 MPa, 8.8 NL/g-cat/h, H_2/CO = 2.5).

described in the experimental section. A group of reference conditions (220 °C, H_2/CO = 2.5, 1.8 MPa, 8.8 NL/g-cat/h) were used at the beginning of the FTS run and following each kinetic period between 272 and 1039 h to assess the extent of deactivation of the Co catalyst. The changes in CO conversion with time are plotted in Fig. 1. CO conversion decreased rapidly in the startup period, losing about 46% of the initial CO conversion (45% → 24.6%) by the time the kinetic experiment started (272 h). Between the kinetic period of 272 and 365 h, CO conversion decreased by an additional 13% (24.6 → 18.9%). However, the catalyst was stable between 365 and 918 h (CO conversions: 18.9–17.5%). In the last 110 h of testing, the deactivation rate of the catalyst increased, CO conversion dropped to 15.5% from 17.5%. Therefore, in order to reduce error in calculating parameter values that could be caused by catalyst deactivation, only the kinetic data recorded during the leveling-off period, where CO conversion decreased only by 1.4%, were used for kinetic parameter estimation. Note that the rapid deactivation in the initial period for cobalt catalysts was also observed in our previous test runs [5,6]. A number of competing possible effects may also be involved, including interior pore filling by high molecular weight wax [28], and changes in cobalt structure [25,29].

3.2. Hydrocarbon distribution at baseline conditions

Changes in CH_4 and C_{5+} hydrocarbon selectivities and the overall hydrocarbon distribution are shown in Fig. 2a and b. Following the rapid activity decline during the first 365 h, an increase in CH_4 (10–12%) and decrease in C_{5+} selectivities (81–78%) were observed (Fig. 2a). During the kinetic period (i.e., 365–918 h), the CH_4 and C_{5+} selectivities remained constant and the overall hydrocarbon distribution changed very little (Fig. 2b). This again suggests that the intrinsic properties of the cobalt catalyst were relatively unchanged during the kinetic period.

3.3. Effect of H_2/CO ratio and CO conversion

The effects of H_2/CO ratio and CO conversion on CH_4 and C_{5+} hydrocarbon selectivities are shown in Fig. 3a and b. In the CO conversion range of 5–60%, a decrease of the H_2/CO ratio from 2.5 to 1.0 resulted in a significant decrease in CH_4 selectivity (12–5%) and an increase in C_{5+} selectivity (78–87%). Note that lower pressures were accompanied by lower H_2/CO ratios, which allows us to deduce that the trend would be more prominent if the same pressure was used at each H_2/CO ratio, since higher pressure generally lowers

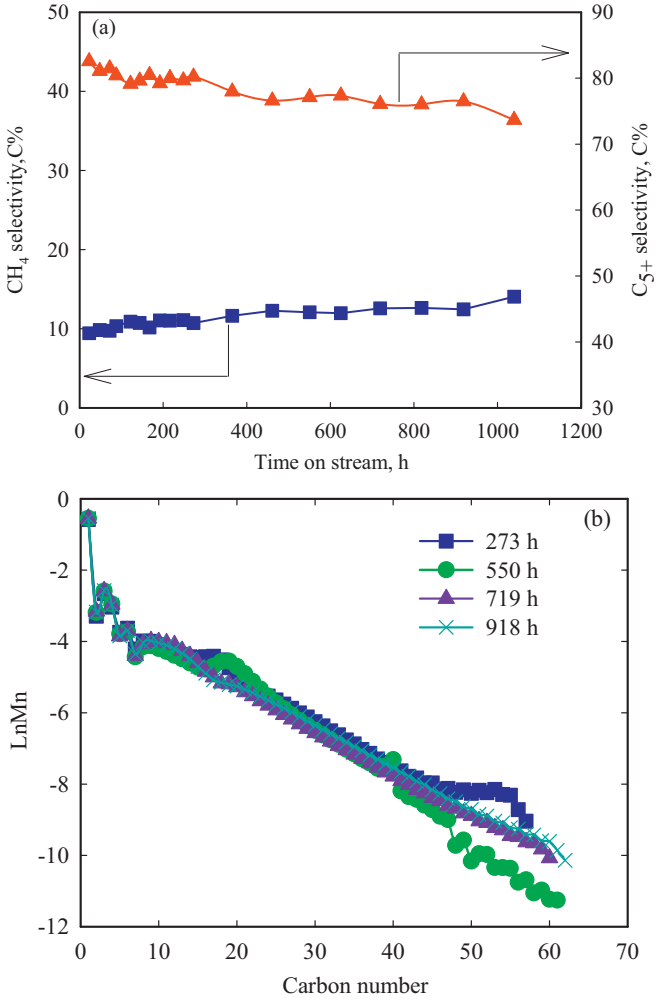

Fig. 2. CH_4 and C_{5+} selectivities as a function of time (a) and ASF distributions (b) under baseline conditions over 25%Co/γ-Al_2O_3 (220 °C, 1.84 MPa, 8.8 NL/g-cat/h, H_2/CO = 2.5).

CH_4 selectivity and enhances C_{5+} selectivity [17]. A decrease in CH_4 selectivity by lowering the H_2/CO ratio can be largely explained by decreases in the hydrogenation rate at lower hydrogen partial pressure and increases in chain growth due to a high coverage of CO [17,21]. Fig. 3a and b suggests that the CH_4 selectivity tends to decrease and the C_{5+} selectivity tends to increase for all H_2/CO ratios as CO conversion was increased. This has been explained by a kinetic water effect [30,31].

3.4. Kinetic results for a Co/Al_2O_3 catalyst

The kinetic parameters for the CAER kinetic model were calculated using the nonlinear least squares fitting method. Thirty-one groups of experimental data were used for the optimization. The kinetic parameter values (220 °C) along with values of statistical parameters, including *F*-values, R^2 value and RMSE for the model, are summarized in Table 2. The reaction orders for partial pressures of CO and H_2 in the FTS kinetic equation were calculated to be −0.31 and 0.88, respectively. This result is close to the values of −0.24 and 0.74 for a pure power law FTS model reported on a Co catalyst by Bartholomew and co-authors [13], but higher than those in our previous studies [5,6], where the reaction orders of hydrogen partial pressure fell in the range of 0.5–0.6. The water effect term was calculated to be −0.24, showing a positive kinetic water effect. This result is different from our previous studies with Co/Al_2O_3 [5,6];

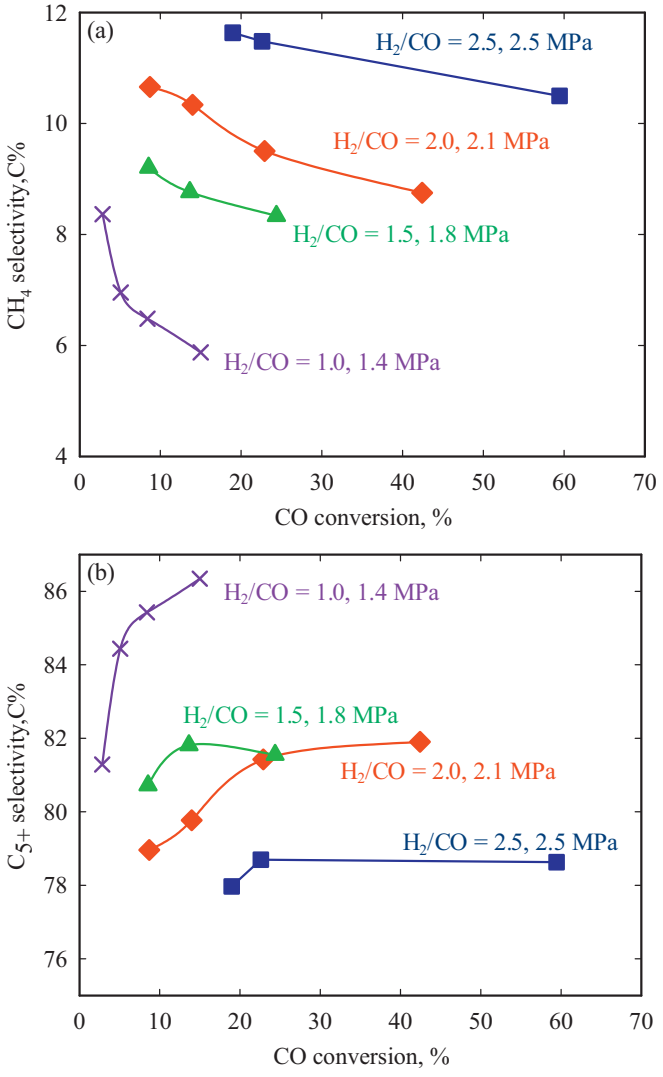

Fig. 3. Effect H_2/CO ratio and CO conversion on the selectivities of CH_4 (a) and C_{5+} (b) at 220 °C.

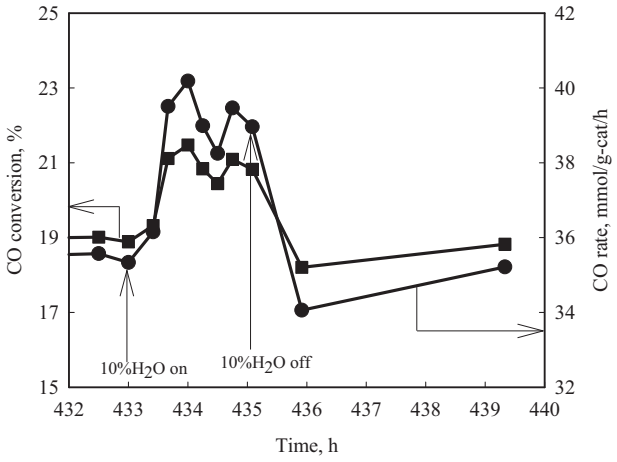

Fig. 4. CO conversion and CO rate before, during, and after adding 10%water over 0.27%Ru-25%Co/Al_2O_3 catalyst. Reaction conditions: 220 °C, H_2/CO = 2.1, syngas pressure = 2.17 MPa (300 psig), and syngas flow = 157.3 NL/h.

however, it is consistent with our water co-feeding results shown in Fig. 4 (Section 3.6), and the recent water co-feeding results for Co/Al_2O_3 reported by Loegdberg et al. [21]. The reason for the difference between our current and previous kinetic results is discussed is this paper.

The negative impact of water obtained in our previous studies for a series of Co/Al_2O_3 catalysts could result from catalyst deactivation (by 50–70%) during the kinetic experiments. Our early kinetic studies primarily focused on examining reversible site suppression caused by H_2O which had been obtained in a previous water co-feeding study [27]; where the reversible water inhibition of FTS was observed after adding 20–30% water to a Pt-Co/Al_2O_3 catalyst. EXAFS/XANES results suggested that the reversible water effect was due to oxidation of Co sites during water addition followed by re-reduction of some oxidized cobalt metal when water addition was terminated [27]. The deactivation rate during the current kinetic experiment was low (1.4% X_{CO}/550 because the catalyst was purposefully evaluated during the stable period following the initial rapid induction period (i.e., the catalyst was significantly aged). Thus, the interference by reversible oxidation of small cobalt crystallites was expected to be decoupled from the kinetics. Therefore, the m value obtained in the current study reflects a kinetic feature of water occurring on stable cobalt particles (i.e., larger aged particles), which is a different kinetic aspect compared to our previous studies.

Based on the CAER model (1), the water effect constant, m, can be derived as follows:

$$m = \frac{[A \times (1 - X_{CO})^a (1 - X_{H_2})^b - X_{CO}](1 - X_{H_2})}{X_{CO}^2} \quad (6)$$

where a and b are reaction orders for the partial pressures of CO and hydrogen, respectively, and X_{CO} and X_{H_2} are conversions of CO and H_2. The combined term A is correlated by the reaction rate constant, initial partial pressures of CO and H_2 and moles of CO at the inlet ($A = kP_{CO,in}^a P_{H_2,in}^b / N_{CO,in}$). From the view of reactor performance, the water effect constant m can be calculated from CO conversion. The real X_{CO} of cobalt catalyst measured at steady state must reflect the nature of the intrinsic water effect. However, when catalyst deactivation occurs due to water oxidation and/or possible water suppression of Co sites as discussed above, the water effect constant, m, value reflected by Eq. (6) would deviate from its actual value and it can become a positive number when conversion decreases to a certain value, which would reflect a negative water effect, since the dominator of Eq. (6) is a quadratic function of CO conversion, and it leads to a more rapid decrease for the dominator value with decreases in CO conversion.

The difference in the reaction orders between this study and the previous studies [5,6] could also be due to different extents of catalyst deactivation in the kinetic studies, since adsorption/dissociation of reactants on a reconstructed Co catalyst surface after deactivation can change. To further explore the hypothesis, we calculated reaction orders of CO and H_2 using the data that include the first five data points with greater deactivation (about 29%), and the reaction orders became −0.23 and 0.98 for P_{CO} and P_{H_2}, respectively, which are different from the values of −0.31 and 0.88 based on the data with little deactivation. Similar results were observed for 11.7%Co/TiO_2 catalyst, as reported by Zennaro et al. [13], where the reaction order for P_{CO} changed from −0.13 to −0.37 when using the data before and after 50% deactivation, respectively.

The reaction orders for P_{CO} and P_{H_2} (−0.32 and 0.88) obtained in this study reflect a mild CO inhibition of the FTS rate and a direct dependence on P_{H_2}. For a better comparison, the effect of partial pressure of P_{H_2} or P_{CO}, with constant P_{CO} or P_{H_2} on the FTS rate is plotted in Fig. 5. At a constant partial pressure of CO (0.7 MPa) or H_2 (1.1 MPa), increasing partial pressure of H_2 (0.66–1.38 MPa) or CO (0.43–0.79 MPa) substantially increases or decreases the FT rate, respectively. Meanwhile, the variations

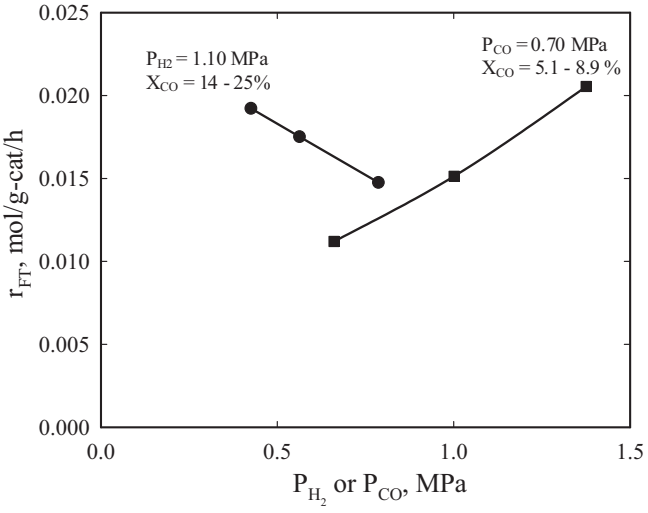

Fig. 5. Change in the FT rate with partial pressure of H_2 or CO over 25%Co/Al_2O_3. Reaction conditions: 220 °C, H_2/CO = 1.0–2.5, and 6.0–16.0 NL/g-cat/h.

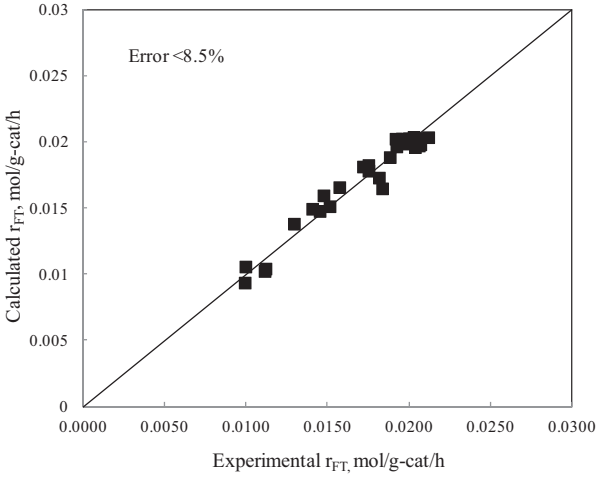

Fig. 6. Parity plot for FT rates based on the CAER FT model.

in H_2 pressure lead to a slightly greater change in the FT rate ($\Delta r_{FT}/\Delta P_{H_2} = 13$ mmol/MPa) than that of variations in CO pressure ($\Delta r_{FT}/\Delta P_{CO} = 12.4$ mmol/MPa), a small difference but in line with the kinetic result.

In comparing mechanistic FT models reported for cobalt catalysts, different reaction orders for P_{H_2} have been reported, but they fall within the range of 0.5–1.5. The reaction order of 0.5 for P_{H_2} in the FTS kinetic model was reported by Sarup et al. [14,15], Bhatelia et al. [20], and Todic et al. [32], while the orders of 1.0 and 1.5 were reported in the models of Yates et al. [16], Anderson et al. [17], Rautavuoma and co-authors [18], and Steen and Schulz [19], respectively. Various types of FTS mechanisms such as carbide, enol or CO insertion have been used to construct kinetic models. Recently, Botes et al. [33] developed a mechanistic FTS kinetic model under a carbide regime. A reaction order for P_{H_2} of 0.75 was obtained by assuming that the first hydrogen addition step to surface active carbon and the second hydrogen addition to surface oxygen are rate determining steps. The second assumption regarding water formation is in line with the study of Ojeda et al. [34], who reported that H-assisted CO dissociation is a dominant mechanism on cobalt (0 0 0 1) surface and that oxygen removal to mainly water is by the controlling step of OH-s + H-s = H_2O + 2s (s being an adsorption site), since the activation energy estimated for this step by density function theory (DFT) is higher than the step O-s + H-s = OH-s + s (62 > 47 kJ/mol). In terms of the reaction order of P_{H_2} (0.88) obtained in this study falling within the range of 0.5–1.5, it is speculated that actual paths leading to chain growth monomer CH_x, may come from more than one rate determining step on cobalt catalyst. Furthermore, the reaction order of 0.88 obtained for P_{H_2} is comparable to the order of 0.75 in the mechanistic model of Botes et al. [33]. This suggests that carbide mechanism may prevail on the cobalt FTS catalyst.

The nature of positive kinetic effect of water as obtained in this study, conducted at low catalyst deactivation, is not well understood. It could be due to water reacting with some type of carbon, e.g. polymeric carbon, on the cobalt surface, resulting in increasing heavier hydrocarbon rates, but not by new pathways arising from the added water [30]. A different perspective, offered by Storsæter et al. [31], is that water may inhibit secondary hydrogenation of primary olefins, so that more olefins are available for insertion and chain growth, leading to a greater selectivity to high molecular weight hydrocarbons. However, these proposed mechanisms cannot explain the fact that water simultaneously reduced the CH_4 rate or the CH_4 selectivity observed in the water co-feeding studies [21,30]. Recently, Bertole et al. [35] used a carbon isotope transient technique to study the effect of water vapor on the reactivity of the surface carbon intermediates involved in FTS on both a supported and an unsupported cobalt catalyst. It was reported that water increases surface active carbon, including the concentration of monomer CH_x used for chain growth by its reacting with adsorbed hydrogen or alkyl species. This explanation appears to be able to more reasonably explain the kinetic water effect results achieved in this study. The reversible negative water effect obtained in our previous kinetic studies [5,6], which were conducted under higher catalyst deactivation rates, and water co-feeding studies [5,27], could be due to cobalt site suppression by water adsorption and size dependent oxidation by water, as discussed previously. For example, as observed by XANES and EXAFS, re-reduction of 25%Co/Al_2O_3 following 25% H_2O addition occurred when H_2O was switched off and led to significant catalyst recovery from the negative effect of water [27]. In this study, reoxidation should be decoupled from the kinetics so that kinetic parameters should be assessed for a metallic cobalt surface.

Table 2 shows that the F value for the CAER Model is only 1.72, smaller than the critical F-value of 3.83 at the 95% confidence level. This suggests that the CAER FT model is adequate to fit the kinetic data. Also, the relatively high correlation coefficient (R^2) value of 0.95 and the small RMSE value of 7.6 E−4 based on the CAER FT model indicate a relatively good fit. Parity plots for the experimental and calculated FT rates, as shown in Table 2 and Fig. 6, provide additional evidence for the goodness of fit of the experimental data by the CAER model. The majority of the points fall on the diagonal for the CAER model, and the residuals for all data points were less than 8.5%.

To verify whether each parameter in the CAER model played a significant role, the T test (student t test) was performed on the kinetic parameters. The results are shown in Table 2 and indicate that absolute T values for all parameters are in the range of the values of 2.9 and 41.6, which is greater than the critical T-value (1.70) at a 95% confidence interval. Thus, based on the T values obtained, all parameters in the CAER model contribute significantly, and a positive kinetic water effect on the FT rate cannot be neglected under the conditions used.

The activation energy (E_a) of the 25%Co/Al_2O_3 catalyst was calculated to be 104 kJ/mol by plotting ln(k) vs. 1/T using several groups of kinetic data collected at 205, 220, 213 and 230 °C (Fig. 7). This result is close to the E_a values of 93–103 kJ/mol reported by Ribeiro et al. [36], and Yates et al. [16]. Withers et al. [37] performed a FTS kinetic study over a 3.5%Co6.6%Zr/SiO_2 catalyst, and

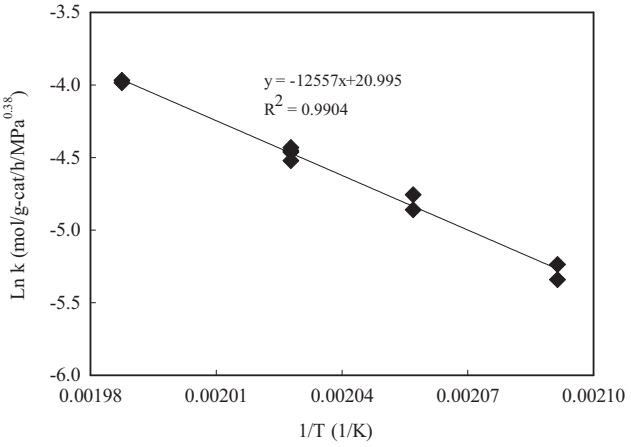

Fig. 7. Arrhenius plot based on CAER FT kinetic model (E_a = 104 kJ/mol).

E_a for FTS was found to be 97 kJ/mol based on the kinetic data collected between 240 and 280 °C. Todic et al. [32,38] recently provided detailed kinetics of FTS over a 0.48%Re–25%Co/Al_2O_3 catalyst. E_a values for C_{2+} paraffins and C_{2+} olefins were found to be 72.4 or 75.5, and 97.2 or 100.4 kJ/mol, respectively, in terms of either a carbide mechanism or a CO insertion mechanism. A recent kinetic and DFT study [34] showed that the E_a for chain initiation for Co catalyst is 92 kJ/mol based on the principle of elementary steps having the lowest energy barrier. Thus, the E_a value obtained in the current work is comparable to the results of these earlier studies.

3.5. Evaluation of FT models for cobalt from literature

In order to examine whether other conventional FT models for Co catalysts can adequately describe our kinetic data, eleven FTS rate expressions for Co catalysts from the literature that are commonly used were selected and these are presented in Table 3. Among them, three are empirical models and they were used by several research groups [8–13], while eight of them are mechanistic ones derived based on either the carbide or enol mechanism [14–20,33]. The kinetic parameters for each FTS model were calculated using the nonlinear regression method. The kinetic parameter values for each model and corresponding statistical values, i.e., *F*-values, R^2 values, and RMSE, are summarized in Table 3.

F values for the power law model (1), and power law models 2 and 3 containing a CO adsorption effect term, yield small *F* values less than 3.6, which is less than the critical *F*-value of 3.8, suggesting that all three empirical models provide a good fit to the data obtained in this study. However, the *F* values for the model of Anderson et al. [17] that is based on the enol mechanism, the model of Yates et al. [16], and that of van Steen and Schulz [19] that is based on the carbide mechanism, were greater than the critical *F*-value, and therefore, had to be rejected. Note that the model of Anderson derived from the enol mechanism included a combined CO and H_2 inhibition term, $P_{H_2}^2 P_{CO}$, and the van Steen model that included a water effect term (i.e., water was assumed to suppress active carbon formation by increasing surface O), led to poor fits. Models 4 and 5 by Sarup et al. [14,15], the models 8 and 10 by Rautavuoma et al. [18] and Bhatelia et al. [20] and that (Model 11) of Botes et al. [33] were all derived from the carbide mechanism, and passed the F test. However, without setting restrictions to kinetic parameters, the values of hydrogen adsorption rate constants obtained in the three models 4, 5 and 10 were negative numbers. Therefore, these three models were rejected as well. Based on the above analysis, among the literature models, only the power law models 1–3 and the mechanistic models 8 and 11 were assumed to adequately describe the kinetic data obtained in this study. Comparing the *F*-values, R^2 values, and RMSE values for these six adequate models, including the CAER model shown in Tables 2 and 3, *F*-values and RMSE values are slightly smaller, and R^2 values is slightly higher. This suggests that the CAER power law model with a small positive water effect is slightly better than others for fitting the kinetic data. It should be mentioned that the

Table 3
Summary of the kinetic examination of FTS models of Co catalyst from open literature.

#	Model	Study	Parameter values				Statistical values		
1	$r_{FT} = kP_{CO}^{a}P_{H_2}^{b}$	[8–11,13]	k, mol/g-cat/h/MPa$^{(a+b)}$	a	b		F^a	R^2	RMSE
			0.0137	−0.35	0.81		2.88	0.92	9.90E−04
2	$r_{FT} = kP_{CO}^{0.65}P_{H_2}^{0.6}/(1+K_1P_{CO})$	[12]	k, mol/g-cat/h/MPa$^{(a+b)}$	K_1, MPa$^{-1.0}$					
			0.6500	41.30			3.58	0.90	1.07E−03
3	$r_{FT} = kP_{CO}P_{H_2}^{0.74}/(1+K_1P_{CO})^2$	[13]	k, mol/g-cat/h/MPa	K_1, MPa$^{-1.0}$					
			0.3080	3.90			2.46	0.93	9.29E−04
4	$r_{FT} = kP_{CO}^{0.5}P_{H_2}^{0.5}/(1+K_1P_{CO}^{0.5}+K_2P_{H_2}^{0.5})^2$	[14,15]	k, mol/g-cat/h/MPa	K_1, MPa$^{-0.5}$	K_2, MPa$^{-0.5}$				
			0.0976	2.36	−0.67		3.05	0.92	1.01E−03
5	$r_{FT} = kP_{CO}P_{H_2}^{0.5}/(1+K_1P_{CO}+K_2P_{H_2}^{0.5})^2$	[14,15]	k, mol/g-cat/h/MPa$^{1.5}$	K_1, MPa$^{-1.0}$	K_2, MPa$^{-0.5}$				
			0.0782	1.95	−0.48		3.47	0.91	1.07E−03
6	$r_{FT} = kP_{CO}P_{H_2}/(1+K_1P_{CO})^2$	[16]	k, mol/g-cat/h/MPa^2	K_1, MPa$^{-1.0}$					
			0.2696	3.61			4.02	0.89	1.17E−03
7	$r_{FT} = kP_{CO}P_{H_2}^2/(1+K_1P_{CO}P_{H_2}^2)$	[17]	k, mol/g-cat/h/MPa^3	K_1, MPa$^{-3.0}$					
			0.1130	4.83			24.50	0.35	2.80E−03
8	$r_{FT} = kP_{CO}^{0.5}P_{H_2}/(1+K_1P_{CO}^{0.5})^3$	[18]	k, mol/g-cat/h/MPa$^{1.5}$	K_1, MPa$^{-0.5}$					
			0.2460	1.65			3.72	0.90	1.13E−03
9	$r_{FT} = k(P_{CO}P_{H_2}^{1.5}/P_{H_2O})/(1+K_1P_{CO}P_{H_2}/P_{H_2O})^2$	[19]	k, mol/g-cat/h/MPa$^{2.0}$	K_1, MPa$^{-1.0}$					
			0.01470	0.19			35.59	0.10	3.39E−03
10	$r_{FT} = kP_{CO}P_{H_2}^{0.5}/(1+K_1P_{CO}+K_2P_{H_2}^{0.5}+mP_{H_2O})^2$	[20]	k, mol/g-cat/h/MPa$^{1.5}$	K_1, MPa$^{-1.0}$	K_2, MPa$^{-0.5}$	m, MPa$^{-1.0}$			
			0.0560	1.61	−0.51	−0.17	3.10	0.920	1.00E−03
11	$r_{FT} = kP_{CO}^{0.5}P_{H_2}^{0.75}/(1+K_1P_{CO}^{0.5})$	[33]	k, mol/g-cat/h/MPa$^{1.25}$	K_1, MPa$^{-0.5}$					
			1.136	8.16			2.85	0.92	1.00E−3

model of Botes et al. (Model 11) also yielded a smaller *F* value, i.e., 2.85, than the other models shown in Table 3, and this apparently means a better fit of the data relative to other empirical and mechanistic models, but just slightly inferior to the model used by CAER shown in Table 2. This result is quite consistent with the discussion in Section 3.4 regarding reaction orders. Considering another mechanistic Model 8 by Rautavuoma et al. [18], developed from a carbide mechanism, also provided a good fit and passed the *F* test (but its *F* value is slightly higher); the kinetic results of the CAER model that gave a better fit again suggests a carbide mechanism prevails in the cobalt catalyzed FTS reaction. This is likely different from the iron catalyst, in which many kinetic studies showed that an enol mechanism was more likely [17,39–43].

The poorest fit results are found for Models 6, 7 and 9 (Table 3), which probably because the models show too strong of a H_2 effect (reaction order ~1.5 and 2.0) and/or too strong of a CO inhibition effect (reaction order ~−1.0). The negative numbers for the H_2 adsorption constant obtained using mechanic Models 4, 5 and 10 should suggest that H_2 adsorption on cobalt surface is rather weak and can be neglected, and that H_2 participates in elemental reactions at a fast rate. This result is in line with recent detail mechanistic studies over cobalt based catalysts [32,44], which estimated that the coverage of the adsorbed H species (θ_H) on the cobalt surface is just less than 1% ($K_{H_2} = \theta_H^2/P_{H_2}$, ~0·0016 MPa^{-1} at 220 °C). The small negative value (−0.17) for the water adsorption term obtained in Model 10 is not expected, but probably suggests a positive water effect. More interesting is that the CO adsorption constant, K_{CO}, for a 25%Co/Al_2O_3 catalyst was estimated to be 8.16 $MPa^{-0.5}$ by fitting the 220 °C data in this study using Model 11 by Botes et al. (Table 3). Since K_{CO} for a commercial Co catalyst with similar catalyst composition, 20%Co–0.05%Pt/Al_2O_3 was reported to be 1.55 $bar^{-0.5}$ (equivalent to 4.9 $MPa^{-0.5}$) at 230 °C by Botes et al. based on the same model [33], the K_{CO} value obtained in this study is certainly logical if one considers that the CO adsorption constant is higher at lower temperatures.

3.6. Water co-feeding study on Ru-Co/Al_2O_3 catalyst

10% H_2O was introduced in a separate run using a Ru promoted 25%Co/Al_2O_3 catalyst at 220 °C after a steady state with a CO conversion of 18.9% was established at 433 h (Fig. 4). Note that the catalyst had been sufficiently aged to improve stability and suppress reversible oxidation, which occurs on small cobalt crystallites (i.e., especially for the fresh catalyst). When water was injected in the reactor with a high inlet gas flow rate (159 NL/h), a new steady state was established after 0.7 h. Water addition was continued for 2 h. CO conversion and FT rate were constant (18.9% and ~35.3 mmol/g-cat/h) before adding 10% H_2O and after the addition of water was terminated, suggesting that the Co catalyst was not significantly altered during adding 10% water between 433 and 435 h. The CO conversion increased to 19.3% and corresponding FT rate increased to 36.2 mmol/g-cat/h after 0.4 h of water addition. They continued to increase to 21% and 39.0 mmol/g-cat/h over the next 0.3 h and these values were maintained until the water flow was cut off at 435 h. To further study the effect of indigenous water on the FTS rate, the kinetic data obtained at the same partial pressures of CO (0.57 MPa) and H_2 (1.0 MPa) were examined, and the results are shown in Fig. 8. As the partial pressure of water inside the reactor increased from 0.08 to 0.41 MPa, the FT rate gradually climbed to 18.8 from 17.2 mmol/g-cat/h. As addressed before, only very little catalyst deactivation was present during water co-feeding and kinetic experiments, and the increased FTS rate by externally added water and indigenous water must therefore reflect a kinetic water effect. Therefore, in the absence of deactivation and/or reversible oxidation by water, the water effect results

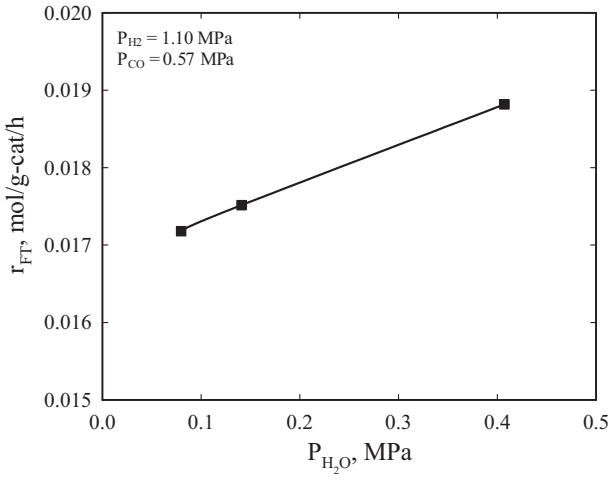

Fig. 8. Effect of indinious water pressure on FT rate over 25%Co/Al_2O_3 catalyst. Reaction conditions: 220 °C, H_2/CO = 2.1, 1.8–2.14 MPa, and 3.0–10.0 NL/g-cat/h.

confirmed a positive kinetic water effect on the FTS rate over the Co/Al_2O_3 catalyst as discussed in Section 3.4.

The effect of water on the selectivities to CH_4 and C_{5+} for cobalt based catalyst has reached a consensus; externally added and indigenous water decrease CH_4 selectivity and increase C_{5+} selectivity [23,30,31,45,46]. However, the effect of water on the FT rate is still under debate. Generally, a positive water effect on the FTS rate was observed on SiO_2 supported Co catalysts [30,31,47], a positive [31] or a slightly negative [48] water effect was observed on Co/TiO_2 catalysts, and a negative [49,50] or no significant effect [23,45] or a positive water effect [21,50] was observed on Co/Al_2O_3 catalyst. The different conclusions drawn on Co/Al_2O_3 or Co/TiO_2 catalysts stem from two opposing roles of water on alumina (or TiO_2) supported cobalt catalyst – a negative effect by deactivation of cobalt or reversible re-oxidation, and a positive kinetic water effect. The reason why the positive kinetic water effect on Co/Al_2O_3 is not easily observed may be explained by rapid reoxidation of small cobalt crystallites (e.g., a reversible kinetic effect) or deactivation (e.g., cobalt support compound formation, sintering, etc.) on Co/Al_2O_3 catalyst that can mask the positive kinetic water effect occurring on stable metallic cobalt particles [21,31]. Water may also contribute to the deactivation of SiO_2 and TiO_2 supported cobalt catalysts, but the extent of deactivation could be much less due to a weaker interaction between these supports and cobalt and by larger cobalt particles presented [27]. Recently, Loegdberg et al. [21] performed a water effect study over a 12%Co–0.5%Re/Al_2O_3 catalyst with a constant syngas partial pressure of 1.4 MPa in a micro fixed-bed reactor, and the space time yield of hydrocarbons was increased from 0.43 to 0.5 g/g-cat/h when 16.8% water was introduced at 80 h. Consequently, it was suggested that the positive water effect on alumina supported cobalt catalyst is related to a change in surface kinetics of FTS. Therefore, the current water effect study is in line with the study of Loegdberg et al. [21]. As noted before, the effect of water in increasing CO reaction rates has been explained by water inducing an acceleration of the CO dissociation and increasing the concentration of surface active carbon for chain growth [35].

4. Conclusions

A kinetic study was conducted over a 25%Co/Al_2O_3 catalyst using a 1-L continuously stirred tank reactor. The following kinetic equation was obtained using the data of 220 °C collected when the

inducted catalyst was stable during the period of 365–918 h under conditions whereby reversible oxidation was avoided.

$$r_{FT} = \frac{0.0133 P_{CO}^{-0.31} P_{H_2}^{0.88}}{(1 - 0.24 P_{H_2O}/P_{H_2})}$$

A positive kinetic water effect on the inducted Co/Al_2O_3 catalyst was obtained under the conditions noted above. The effects of externally added and indigenous water on the FTS on an unpromoted and a Ru-promoted Co/Al_2O_3 were also studied in this paper. The results from the water effect studies are in line with a positive kinetic water effect on stable inducted cobalt particles.

The effect of reversible reoxidation and catalyst deactivation on Co and the reversible reoxidation of Co in water co-feeding experiments on FTS kinetics was discussed in this paper. Catalyst deactivation and/or oxidation likely alters the adsorption/dissociation behavior of reactants on the catalyst surface, and consequently, the reaction orders. When, for example, a fresh catalyst is used having smaller cobalt crystallites that are susceptible to reoxidation (and irreversible deactivation as well), an increase is observed in the water effect constant, and can change the positive kinetic water effect to a negative one based on the CAER empirical model.

Eleven more classical FT models (empirical and mechanistic models) for cobalt catalysts obtained from the open literature were evaluated. Five of them (three empirical and two mechanistic models) yielded meaningful values and adequately described the kinetic data of $25\%Co/Al_2O_3$. The Model of Botes et al. based on a carbide mechanism also gave a better fit of the leveling off data collected at 220 °C but was slightly inferior to the CAER empirical model. The current empirical kinetic model and results suggest that a carbide mechanism prevails for the cobalt catalyst.

Acknowledgments

This work was supported by NASA contract, NNX07AB93A and the Commonwealth of Kentucky.

References

[1] E. Iglesia, Appl. Catal. A: Gen. 161 (1997) 59.
[2] E. van Steen, M. Claeys, Chem. Eng. Technol. 31 (2008) 655.
[3] O. Borg, N. Hammer, B.C. Enger, R. Myrstad, O.A. Lindv, S. Eri, T.H. Skagseth, E. Rytter, J. Catal. 279 (2011) 163.
[4] B.H. Davis, DOE final report, 2002.
[5] T.K. Das, X.D. Zhan, J. Li, G. Jacobs, M.E. Dry, B.H. Davis, Stud. Surf. Sci. Catal. 163 (2007) 289.
[6] W. Ma, G. Jacobs, D.E. Sparks, M.K. Gnanamani, V.R.R. Pendyala, C.H. Yen, J.L.S. Klettlinger, T.M. Tomsik, B.H. Davis, Fuel 90 (2011) 756.
[7] W. Ma, G. Jacobs, B.H. Davis, NASA final report, 2011.
[8] C.H. Yang, F.E. Massoth, A.G. Oblad, Adv. Chem. Ser. 178 (1979) 35.
[9] J. Wang, Ph.D. Thesis, Brigham Young University, Provo, UT, 1987.
[10] R.B. Pannell, C.L. Kibby, T.P. Kobylinski, Proc. 7th Inter. Cong. Catal. Tokyo, 1980, p. 447.
[11] C.S. Kellner, A.T. Bell, J. Catal. 70 (1981) 418.
[12] E. Iglesia, S.C. Reyes, S.L. Soled, in: R.E. Becker, C.J. Pereira (Eds.), Reaction-transport Selectivity Models and the Design of Fischer–Tropsch Catalysts in Computer-aided Design of Catalysts, Marcel Dekker, New York, 1993.
[13] R. Zennaro, M. Tagliabue, C.H. Bartholomew, Catal. Today 58 (2000) 309.
[14] B. Sarup, B.W. Wojciechowski, Can. J. Chem. Eng. 67 (1989) 62.
[15] B.W. Wojciechowski, Catal. Rev. Sci. Eng. 30 (1988) 629.
[16] I.C. Yates, C.N. Satterfield, Energy Fuels 5 (1991) 168.
[17] R.B. Anderson, in: P.H. Emmett (Ed.), Catalysis, vol. 4, Reinhold, New York, 1956.
[18] A. Outi, I. Rautavuoma, H.S. van der Baan, Appl. Catal. 1 (1981) 247.
[19] E. van Steen, H. Schulz, Appl. Catal. A: Gen. 186 (1999) 309.
[20] T. Bhatelia, W. Ma, G. Jacobs, B.H. Davis, D.B. Bukur, Chem. Eng. Trans. 25 (2011) 707.
[21] S. Loegdberg, M. Boutonnet, J.C. Walmsley, S. Jaeras, A. Holmen, E.A. Blekkan, Appl. Catal. A: Gen. 393 (2011) 109.
[22] G.P. van der Laan, A.A.C.M. Beenackers, Catal. Rev. Sci. Eng. 41 (1999) 255.
[23] F.G. Botes, Ind. Eng. Chem. Res. 48 (2009) 1859.
[24] N.E. Tsakoumis, M. Rønning, O. Borg, E. Rytter, A. Holmen, Catal. Today 154 (2010) 162.
[25] A.M. Saib, D.J. Moodley, I.M. Ciobica, M.M. Hauman, B.H. Sigwebela, C.J. Weststrate, J.W. Niemantsverdriet, J. van de Loosdrecht, Catal. Today 154 (2010) 271.
[26] H. Karaca, O.V. Safonova, S. Chambrey, P. Fongarland, P. Roussel, A. Griboval-Constant, M. Lacroix, A.Y. Khodakov, J. Catal. 277 (2011) 14.
[27] G. Jacobs, P.M. Patterson, T.K. Das, M. Luo, B.H. Davis, Appl. Catal. A: Gen. 270 (2004) 65.
[28] V.R.R. Pensyala, G. Jacobs, M. Luo, B.H. Davis, Catal. Lett. 143 (2013) 395.
[29] G. Jacobs, W. Ma, P. Gao, B. Todic, T. Bhatelia, D.B. Bukur, B.H. Davis, Catal. Today 214 (2013) 100.
[30] S. Krishnamoorthy, M. Tu, M.P. Ojeda, D. Pinna, E. Iglesia, J. Catal. 211 (2002) 422.
[31] S. Storsæter, O. Borg, E.A. Blekkan, A. Holmen, J. Catal. 231 (2005) 405.
[32] B. Todic, W.P. Ma, G. Jacobs, B.H. Davis, B.D. Bukur, Catal. Today (2013), http://dx.doi.org/10.1016/j.cattod.2013.10.014.
[33] F.G. Botes, B. van Dyk, C. McGregor, Ind. Eng. Chem. Res. 48 (2009) 10439.
[34] M. Ojeda, R. Nabar, A.U. Nilekar, A. Ishikawa, M. Mavrikakis, E. Iglesia, J. Catal. 272 (2010) 287.
[35] C.J. Bertole, C.A. Mims, G. Kiss, J. Catal. 210 (2002) 84.
[36] F.H. Ribeiro, A.E. Schach von Wittenau, C.H. Bartholomew, G.A. Somorjai, Catal. Rev. Sci. Eng. 39 (1997) 49.
[37] H.P. Withers, K.F. Eliezer, J.W. Mitchell, Ind. Eng. Chem. Res. 29 (1990) 1807.
[38] B. Todic, T. Bhatelia, G.F. Froment, W.P. Ma, G. Jacobs, B.H. Davis, D.B. Bukur, Ind. Eng. Chem. Res. 52 (2013) 669.
[39] Z.T. Liu, Y.W. Li, J.L. Zhou, B.J. Zhang, J. Chem. Soc. Faraday Trans. 91 (1995) 3255.
[40] M.E. Dry, T. Shingles, L.J. Boshoff, J. Catal. 25 (1972) 99.
[41] S. Ledakowicz, H. Nettelhoff, R. Kokuun, W.D. Deckwer, Ind. Eng. Chem. Process Des. Dev. 24 (1985) 1043.
[42] G.A. Huff Jr., C.N. Satterfield, Ind. Eng. Chem. Process Des. Dev. 23 (1984) 696.
[43] W.J. Shen, J.L. Zhou, B.J. Zhang, J. Nat. Gas Chem. 3 (1994) 385.
[44] C.G. Visconti, E. Tronconi, L. Lietti, P. Forzatti, S. Rossini, R. Zennaro, Top. Catal. 54 (2011) 786.
[45] H. Schulz, M. Claeys, S. Harms, Stud. Surf. Sci. Catal. 107 (1997) 193.
[46] W.P. Ma, G. Jacobs, Y. Ji, T. Bhatelia, D.B. Bukur, S. Khalid, B.H. Davis, Top. Catal. 54 (2011) 757.
[47] J.L. Li, G. Jacobs, T.K. Das, Y.Q. Zhang, B.H. Davis, Appl. Catal. 236 (2002) 67.
[48] J.L. Li, G. Jacobs, T.K. Das, B.H. Davis, Appl. Catal. 233 (2002) 255.
[49] J.L. Li, X.D. Zhan, Y.Q. Zhang, G. Jacobs, T. Das, B.H. Davis, Appl. Catal. 228 (2002) 203.
[50] O. Borg, S. Storsæter, S. Eri, H. Wigum, E. Rytter, A. Holmen, Catal. Lett. 107 (2006) 95.